UDC 539. 4

Application of the Micropolar Theory to the Strength Analysis of Bioceramic Materials for Bone Reconstruction

V. A. Eremeyev, A. Skrzat, and A. Vinakurava

Rzeszów University of Technology, Rzeszów, Poland

The application of the linear micropolar theory to the strength analysis of bioceramic materials for bone reconstruction is described. Micropolar elasticity allows better results to be obtained for microstructural and singular domains as compared to the classical theory of elasticity. The fundamental equations of the Cosserat continuum are cited. The description of FEM implementation of micropolar elasticity is given. The results of solving selected 3D test problems are presented. Comparison of classical and micropolar solutions is discussed.

Keywords: Cosserat continuum, micropolar elasticity, stress concentration, finite element analysis, porous media, bones.

Introduction. Bones, bones with implants, and their modeling within the framework of continuum mechanics constitute a very challenging problem due to the complex microstructure, material properties, physical and chemical processes [1, 2]. Among many problems related to the bone modeling, the bone reconstruction with porous implants is one of the most important from the practical and theoretical points of view [3–8].

Mesoporous biomaterials allow for the regeneration of a bone tissue in the treatment of various pathologies [9]. Porosity necessary for the bone regeneration has been shown by Kuboki using solid and porous particles of hydroxyapatite for BMP-2 delivery. It is important that any new bone was not formed on solid particles, while in the porous scaffolds direct osteogenesis occurred [10]. The analysis of such materials is an elaborate procedure since their microstructure should be taken into account.

Reliable numerical analysis of bones and biomaterials is a very complicated task mostly because of their complex geometry. In practice, only small representative volume elements can be examined. Indeed, a trabecular bone can be considered a porous solid with a highly nonuniform microstructure (Fig. 1). For the bone modeling, different mechanical models were proposed. Among them, poroelasticity [3, 4], media with internal variables [5–8] should be mentioned. In some cases a bone can be treated as an open foam-like structure or a system of beams. Since in foam struts or in beams not only forces but also moments exist, this naturally leads to the model of the Cosserat continuum, also termed micropolar elasticity [11, 12]. Within the micropolar media model normal and tangential surface tractions are considered, but unlike classical elasticity we also take into account moment interactions and microrotations of material particles. So, we may replace the real bone structure with an equivalent homogeneous micropolar solid (Fig. 1). This replacement may significantly reduce the computational efforts with sufficient accuracy in comparison with the real bone structure or beam lattice. The idea of applying the Cosserat continuum model to the bone modeling relates to the original studies by Lakes and coworkers [13–16] where a few experiments on porous materials, including bones, were performed. Recently, in [17–19] the homogenization technique leading to micropolar elasticity as applied to bones has been developed. In the latter publications the material parameters of micropolar elasticity are derived. It should also be noted that such materials, as foams, porous media, beam lattices may bring to more general models of continuum mechanics [20–23].

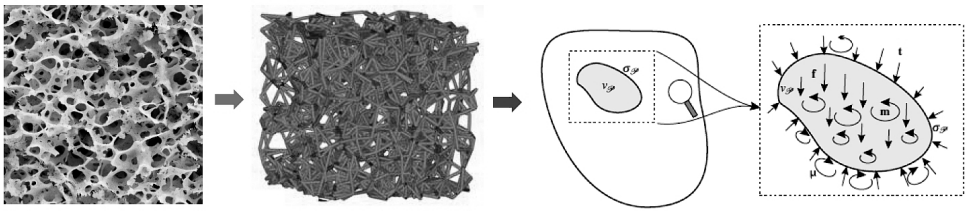

Fig. 1. Real bone structure, the beam lattice, and homogeneous micropolar media representations.

This study covers the following issues. The basic equations of linear isotropic micropolar elasticity are first recalled. Emphasis is given to the constitutive relations for the bone modeling. In the second section, the finite element technique is presented, which would be used for the calculations of a few problems in the next section. Here the stress concentration problems in the vicinity of notches and holes of various sizes would be analyzed.

Basic Equations of Micropolar Elasticity. Within micropolar continuum mechanics, apart from the field of translations, the local rotations of material particles of a deformable body and their moment interactions are taken into account as the additional degrees of freedom. Following Eringen [11], the strain measures are introduced, being the linear stretch tensor and bending-torsion tensor, also termed the wryness tensor

$$\varepsilon_{ij} = u_{j,i} + e_{ijk}\theta_k, \tag{1}$$

$$\kappa_{ij} = \theta_{i,j}, \tag{2}$$

where u_j is the vector of translations, θ_j is the vector of microrotations, e_{ijk} is the Levi-Civita symbol, $i, j, k = 1, 2, 3$. Hereinafter we use the Einstein summation rule over repeating indices. Due to the contribution of microrotations, the tensors ε_{ij} and κ_{ij} are asymmetric. In the micropolar theory, the stress measures are the stress tensor σ_{ji} (force per unit area) and coupled stress tensor m_{ji} (moment per unit area).

In the absence of body forces and moments, the equilibrium equations of the Cosserat continuum take the form

$$\sigma_{ji,j} = 0, \tag{3}$$

$$m_{ji,j} + e_{imn}\sigma_{mn} = 0. \tag{4}$$

It is worthy of emphasis that the stress tensors are also asymmetric and strains (1), (2) and (3), (4) are energy-related.

Further the Voigt notation is applied. So the micropolar stress and strain tensors have the following generalized form:

$$\{\sigma_M\} = \begin{Bmatrix}\sigma \\ m\end{Bmatrix}, \qquad \{\varepsilon_M\} = \begin{Bmatrix}\varepsilon \\ \kappa\end{Bmatrix}, \tag{5}$$

where the vectors are introduced

$$\sigma = \{\sigma_{xx}, \sigma_{yy}, \sigma_{zz}, \sigma_{xy}, \sigma_{yx}, \sigma_{yz}, \sigma_{zy}, \sigma_{xz}, \sigma_{zx}\}^T, \tag{6}$$

$$m = \{m_{xx}, m_{yy}, m_{zz}, m_{xy}, m_{yx}, m_{yz}, m_{zy}, m_{xz}, m_{zx}\}^T, \tag{7}$$

$$\varepsilon = \{\varepsilon_{xx}, \varepsilon_{yy}, \varepsilon_{zz}, \varepsilon_{xy}, \varepsilon_{yx}, \varepsilon_{yz}, \varepsilon_{zy}, \varepsilon_{xz}, \varepsilon_{zx}\}^T, \tag{8}$$

$$\kappa = \{\kappa_{xx}, \kappa_{yy}, \kappa_{zz}, \kappa_{xy}, \kappa_{yx}, \kappa_{yz}, \kappa_{zy}, \kappa_{xz}, \kappa_{zx}\}^T. \tag{9}$$

With this notation, the constitutive equations of the Cosserat medium are defined as

$$\{\sigma_M\} = [C]\{\varepsilon_M\}, \tag{10}$$

where the stiffness matrix $[C]$ consists of the following submatrices:

$$[C] = \begin{bmatrix} A & 0 \\ 0 & B \end{bmatrix}. \tag{11}$$

In the isotropic case the matrix $[A]$ is given by the formula [11, 12, 24, 25]:

$$A = \begin{bmatrix} \lambda+2\mu+\kappa & \lambda & \lambda & & & & & & & & \\ \lambda & \lambda+2\mu+\kappa & \lambda & & & & & & & & \\ \lambda & \lambda & \lambda+2\mu+\kappa & & & & & & & & \\ & & & \mu+\kappa & \mu & & & & & & \\ & & & \mu & \mu+\kappa & & & & & & \\ & & & & & \mu+\kappa & \mu & & & & \\ & & & & & \mu & \mu+\kappa & & & & \\ & & & & & & & \mu+\kappa & \mu & & \\ & & & & & & & \mu & \mu+\kappa & & \\ & & & & & & & & & & \end{bmatrix}, \tag{12}$$

and the matrix $[B]$ has a similar structure:

$$[B] = \begin{bmatrix} \alpha+\beta+\gamma & \alpha & \alpha & & & & & & \\ \alpha & \alpha+\beta+\gamma & \alpha & & & & & & \\ \alpha & \alpha & \alpha+\beta+\gamma & & & & & & \\ & & & \gamma & \beta & & & & \\ & & & \beta & \gamma & & & & \\ & & & & & \gamma & \beta & & \\ & & & & & \beta & \gamma & & \\ & & & & & & & \gamma & \beta \\ & & & & & & & \beta & \gamma \end{bmatrix}. \tag{13}$$

In (12) and (13) only nonzero elements λ, μ, κ are shown up, and α, β, γ are the elastic moduli discussed below. Six engineering moduli for the isotropic case and their values for bones [13–16] are cited in Table 1. These values were found through predicted relations between material properties and specimen sizes within the micropolar elasticity size-effect. Thus, there are theoretically two characteristic length parameters for torsion and bending, which can be determined from experimental data.

T a b l e 1

Micropolar Material Characteristics for Bones

Characteristic	Symbol	Value
Shear modulus (MPa)	G	4000
Poisson's ratio	ν	0.25
Coupling number	N	≥ 0.5
Characteristic length (torsion) (m)	l_t	0.00022
Characteristic length (bending) (m)	l_b	0.00045
Polar ratio	Ψ	1.5

The first three parameters are related to λ, μ, κ as

$$\begin{cases} G = \dfrac{2\mu + \kappa}{2}, \\ \nu = \dfrac{\lambda}{2\lambda + 2\mu + \kappa}, \\ N^2 = \dfrac{\kappa}{2(\mu + \kappa)}. \end{cases} \tag{14}$$

Solving the system of equations (14) for λ, μ, κ, we obtain

$$\begin{cases} \kappa = \dfrac{2GN^2}{1 - N^2}, \\ \mu = G\left(1 - \dfrac{N^2}{1 - N^2}\right), \\ \lambda = \dfrac{2G\nu}{1 - 2\nu}. \end{cases} \tag{15}$$

The next three material moduli α, β, γ depend on l_t, l_b, Ψ via relations

$$\begin{cases} l_t^2 = \dfrac{\beta + \gamma}{2\mu + \kappa}, \\ l_b^2 = \dfrac{\gamma}{2(2\mu + \kappa)}, \\ \Psi = \dfrac{\beta + \gamma}{\alpha + \beta + \gamma}. \end{cases} \tag{16}$$

Solving the system of equations (16) in terms of α, β, γ, we find

$$\begin{cases} \alpha = l_t^2 (2\mu + \kappa)(1 - \Psi)/\Psi, \\ \beta = (l_t^2 - 2l_b^2)(2\mu + \kappa), \\ \gamma = 2l_b^2 (2\mu + \kappa). \end{cases} \tag{17}$$

The 8-Node Hybrid Micropolar Isoparametric Element. For strength analysis based on micropolar elasticity, the 8-node hexahedral element is constructed. The element is represented in the Cartesian and natural coordinates (Fig. 2).

For the interpolation of displacements and microrotations the same shape functions are used. The *i*th shape function is defined as

$$N_i(\xi, \eta, \mu) = \frac{1}{8}(1+\xi\xi_i)(1+\eta\eta_i)(1+\mu\mu_i). \tag{18}$$

The stiffness matrix of the element is given by

$$k = \int_V D^T C D dV, \tag{19}$$

where the matrix C is defined in (11)–(13) and matrix D is the matrix of shape function derivatives viz. the relation between the Erringen strains and nodal displacements and microrotations,

$$\begin{Bmatrix} \varepsilon_{xx} \\ \varepsilon_{yy} \\ \varepsilon_{zz} \\ \varepsilon_{xy} \\ \varepsilon_{yx} \\ \varepsilon_{yz} \\ \varepsilon_{zy} \\ \varepsilon_{xz} \\ \varepsilon_{zx} \\ \kappa_{xx} \\ \kappa_{yy} \\ \kappa_{zz} \\ \kappa_{xy} \\ \kappa_{yx} \\ \kappa_{yz} \\ \kappa_{zy} \\ \kappa_{xz} \\ \kappa_{zx} \end{Bmatrix} = \begin{bmatrix} f_{1,x} & 0 & 0 & 0 & 0 & 0 & \dots & f_{8,x} & 0 & 0 & 0 & 0 & 0 \\ 0 & f_{1,y} & 0 & 0 & 0 & 0 & \dots & 0 & f_{8,y} & 0 & 0 & 0 & 0 \\ 0 & 0 & f_{1,z} & 0 & 0 & 0 & \dots & 0 & 0 & f_{8,z} & 0 & 0 & 0 \\ 0 & f_{1,x} & 0 & 0 & 0 & f_1 & \dots & 0 & f_{8,x} & 0 & 0 & 0 & f_8 \\ f_{1,y} & 0 & 0 & 0 & 0 & -f_1 & \dots & f_{8,y} & 0 & 0 & 0 & 0 & -f_8 \\ 0 & 0 & f_{1,y} & f_1 & 0 & 0 & \dots & 0 & 0 & f_{8,y} & f_8 & 0 & 0 \\ 0 & f_{1,z} & 0 & -f_1 & 0 & 0 & \dots & 0 & f_{8,z} & 0 & -f_8 & 0 & 0 \\ 0 & 0 & f_{1,x} & 0 & -f_1 & 0 & \dots & 0 & 0 & f_{8,x} & 0 & -f_8 & 0 \\ f_{1,z} & 0 & 0 & 0 & f_1 & 0 & \dots & f_{8,z} & 0 & 0 & 0 & f_8 & 0 \\ 0 & 0 & 0 & f_{1,x} & 0 & 0 & \dots & 0 & 0 & 0 & f_{8,x} & 0 & 0 \\ 0 & 0 & 0 & 0 & f_{1,y} & 0 & \dots & 0 & 0 & 0 & 0 & f_{8,y} & 0 \\ 0 & 0 & 0 & 0 & 0 & f_{1,z} & \dots & 0 & 0 & 0 & 0 & 0 & f_{8,z} \\ 0 & 0 & 0 & f_{1,y} & 0 & 0 & \dots & 0 & 0 & 0 & f_{8,y} & 0 & 0 \\ 0 & 0 & 0 & 0 & f_{1,x} & 0 & \dots & 0 & 0 & 0 & 0 & f_{8,1} & 0 \\ 0 & 0 & 0 & 0 & f_{1,z} & 0 & \dots & 0 & 0 & 0 & 0 & f_{8,z} & 0 \\ 0 & 0 & 0 & 0 & 0 & f_{1,y} & \dots & 0 & 0 & 0 & 0 & 0 & f_{8,y} \\ 0 & 0 & 0 & f_{1,z} & 0 & 0 & \dots & 0 & 0 & 0 & f_{8,z} & 0 & 0 \\ 0 & 0 & 0 & 0 & 0 & f_{1,x} & \dots & 0 & 0 & 0 & 0 & 0 & f_{8,x} \end{bmatrix} \begin{Bmatrix} u_x^1 \\ u_y^1 \\ u_z^1 \\ \theta_x^1 \\ \theta_y^1 \\ \theta_z^1 \\ \dots \\ u_x^8 \\ u_y^8 \\ u_z^8 \\ \theta_x^8 \\ \theta_y^8 \\ \theta_z^8 \end{Bmatrix}. \tag{20}$$

Integration in (19) is over the element volume presented as the loop of the Gaussian points. The $2\times2\times2$ Gaussian quadrature is used.

Test Problems. The finite element method program elaborated for solving the 3D problems of micropolar elasticity has to be verified and validated in several test ones. The two examined problems, including singularities are presented in Fig. 3. This choice is stemming from more pronounced micropolar properties in a singular case [26–28]. Test problems are solved for different a, b, d, and h dimensions and mesh densities. Two types of loads are considered: constant pressure (replaced with kinematically equivalent forces) or displacement applied to the right-hand lateral (edge) surface (kinematic load).

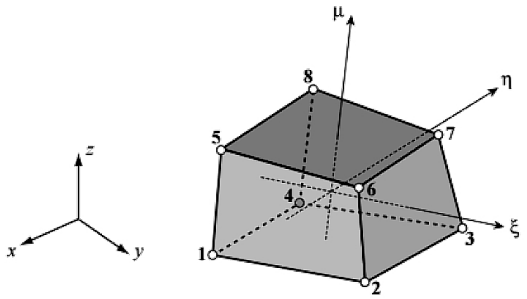

Node	ξ	η	μ
1	−1	−1	−1
2	+1	−1	−1
3	+1	+1	−1
4	−1	+1	−1
5	−1	−1	+1
6	+1	−1	+1
7	+1	+1	+1
8	−1	+1	+1

Fig 2. The 8-node hexahedral element.

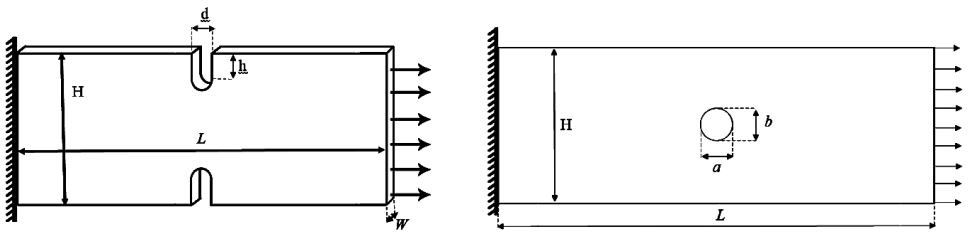

Fig. 3. Examined test problems.

As is known, classical elasticity is a special case of micropolar elasticity with fixed microrotations (equal zero). The results of solving test problems using micropolar software, wherein all microrotations are fixed, are compared with those obtained through commercial software. An alternative opportunity to obtain classical elasticity solutions is the employment of only two first material characteristics from Table 1, if all remaining data are taken as zero.

In the test problems the effect of mesh density on the body response was investigated. The symmetry of obtained solutions was checked (problems can be solved more efficiently in terms of double symmetry).

As an example, the following dimensions: $L = 0.03$ m and $H = 0.01$ m are given in Fig. 4. The other parameters were varied, e.g., over the range of 0.001–0.0005 m for the diameter d and of 0.0003–0.001 m for the minor axis a of the ellipse. Such dimensions are chosen for evaluating the impact of the characteristic length in the micropolar media.

Finite element meshes (Fig. 4) are generated with commercial software (ANSYS or ABAQUS). The maximum size of test problems is 120 thousand degrees of freedom. As mentioned above, micropolar elasticity provides the same solutions as the classical theory of elasticity if all microrotations are fixed or if only two material characteristics are used (shear or Young's modulus and Poisson's ratio). Solutions obtained with commercial software (classical theory of elasticity) and elaborated software are compared in Figs. 5 and 6. As can be seen, stress distributions and magnitudes (not shown for micropolar software) converge excellently. It proves that the results, obtained with elaborated software in terms of micropolar elasticity and reduced to the classical one, are reliable. The results of micropolar analysis are processed with a specially developed OpenGL library-based program.

As expected, the whole family of test problems solved so far confirmed that the coupled stresses appear only in the vicinity of singularities. In other cases the solutions obtained in terms of micropolar and classical elasticity are comparable. The distribution of the m_{zz} stresses (axis z is normal to the plate) in the plate with a sharp notch is given in Fig. 7. In this test problem the magnitude of coupled stresses (all components) is a few orders lower than, e.g., the magnitude of a longitudinal stress component.

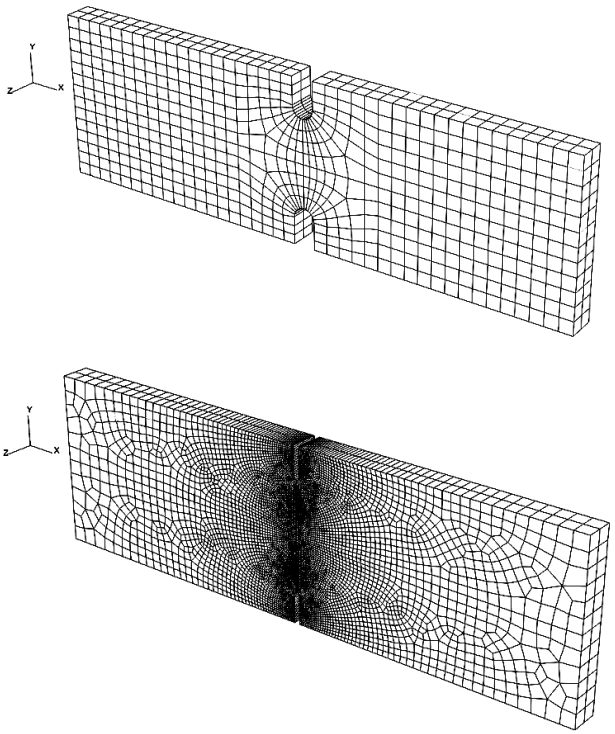

Fig. 4. Examples of coarse and fine meshes.

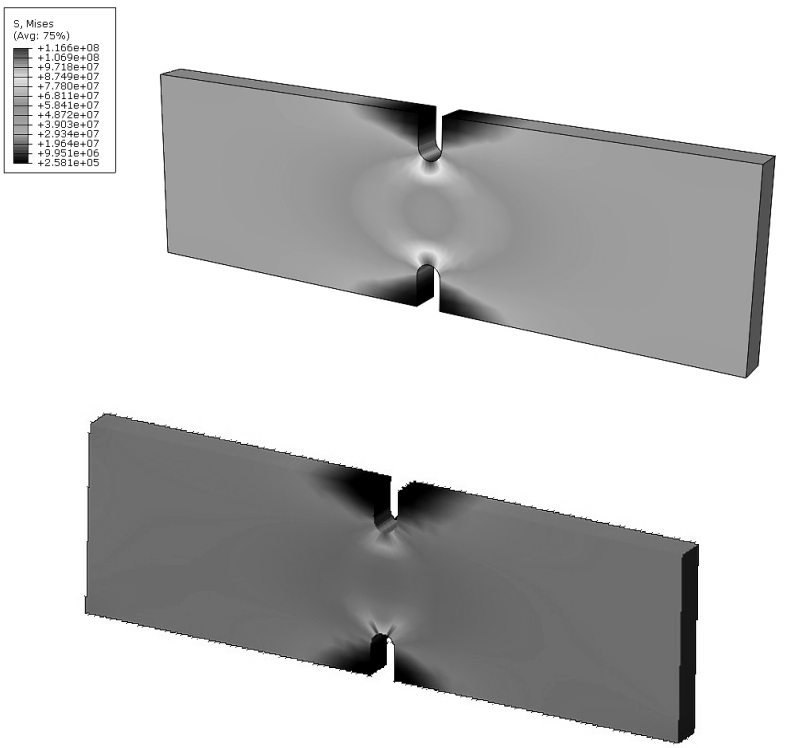

Fig. 5. Comparison of von Mises stresses (Pa) obtained with commercial (top) and elaborated software (bottom).

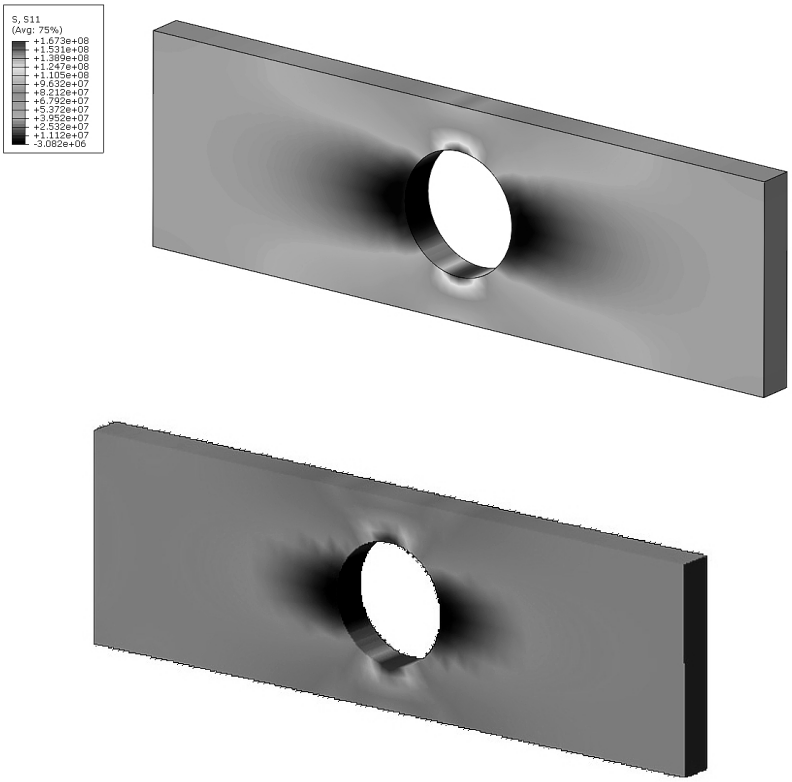

Fig. 6. Comparison of longitudinal stresses (Pa) obtained with commercial (top) and elaborated software (bottom).

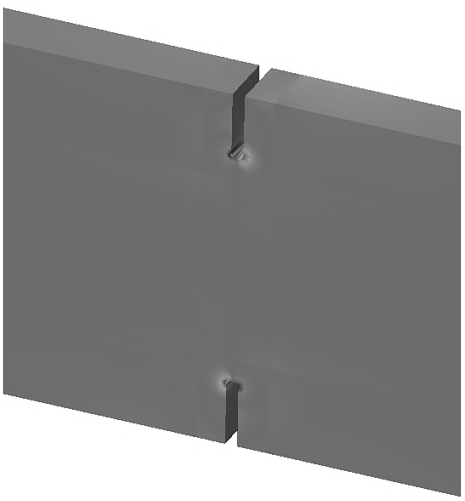

Fig. 7. Distribution of the m_{zz} stresses in the plate with a sharp notch.

Conclusions. Micropolar elasticity as one of the models for the materials with a complex microstructure is used for the bone modeling. The micropolar, elasticity is a very effective tool for solving the singular problems and the problems for microstructure-containing domains, like in foams and bones. For numerical analysis specific finite elements were constructed and implemented in commercial software. An excellent convergence has

been achieved for all test problems. The results obtained within micropolar elasticity are compared with classical linear one. Numerical tests demonstrated that coupled stresses appeared in the vicinity of singularities. So the effect of micropolar properties is related to the notches and holes with the size of the same order as the characteristic length parameters of micropolar elasticity.

Acknowledgments. The research received funding from the People Program (Marie Curie ITN transfer) of the European Union's Seventh Framework Programme for research, technological development and demonstration under grant agreement No. PITN-GA-2013-606878.

1. S. Cowin (Ed.), *Bone Mechanics Handbook*, CRC Press, Boca Raton, FL (2001).
2. Y. H. An and R. A. Draughn (Eds.), *Mechanical Testing of Bone and the Bone–Implant Interface*, CRC Press, Boca Raton, FL (2000).
3. S. C. Cowin and D. H. Hegedus, "Bone remodeling I: theory of adaptive elasticity," *J. Elasticity*, **6**, No. 3, 313–326 (1976).
4. D. H. Hegedus and S. C. Cowin, "Bone remodeling II: small strain adaptive elasticity," *J. Elasticity*, **6**, No. 4, 337–352 (1976).
5. T. Lekszycki and F. dell'Isola, "A mixture model with evolving mass densities for describing synthesis and resorption phenomena in bones reconstructed with bio-resorbable materials," *Z. Angew. Math. Mech*, **92**, No. 6, 426–444 (2012).
6. I. Giorgio, U. Andreaus, D. Scerrato, and F. dell'Isola, "A visco-poroelastic model of functional adaptation in bones reconstructed with bio-resorbable materials," *Biomech. Model. Mechanobiol.*, **15**, No. 5, 1325–1343 (2016).
7. I. Giorgio, U. Andreaus, D. Scerrato, and P. Braidotti, "Modeling of a non-local stimulus for bone remodeling process under cyclic load: Application to a dental implant using a bioresorbable porous material," *Math. Mech. Solids* (2016), DOI: 10.1177/1081286516644867.
8. I. Giorgio, U. Andreaus, T. Lekszycki, and A. Della Corte, "The influence of different geometries of matrix/scaffold on the remodeling process of a bone and bio-resorbable material mixture with voids," *Math. Mech. Solids* (2015), DOI: 10.1177/1081286515616052.
9. M. Vallet-Regi, I. Izquierdo-Barba, and M. Colilla, "Structure and functionalization of mesoporous bioceramics for bone tissue regeneration and local drug delivery," *Phil. Trans. R. Soc. A*, **370**, 1400–1421 (2012).
10. V. Karageorgiou and D. Kaplan, "Porosity of 3D biomaterial scaffolds and osteogenesis," *Biomaterials*, **26**, 5474–5491 (2005).
11. A. C. Eringen, *Microcontinuum Field Theories: I. Foundations and Solids*, Springer-Verlag, New York (1999).
12. V. A. Eremeyev, L. P. Lebedev, and H. Altenbach, F*oundations of Micropolar Mechanics*, Springer, Berlin (2013).
13. J. F. C. Yang and R. S. Lakes, "Experimental study of micropolar and couple stress elasticity in compact bone in bending," *J. Biomech.*, **15**, No. 2, 91–98 (1982).
14. H. C. Park and R. S. Lakes, "Cosserat micromechanics of human bone: strain redistribution by a hydration sensitive constituent," *J. Biomech.*, **19**, No. 5, 385–397 (1986).
15. R. S. Lakes, "Experimental microelasticity of two porous solids," *Int. J. Solids Struct.*, **22**, No. 1, 55–63 (1986).

16. R. S. Lakes, "Experimental micro mechanics methods for conventional and negative Poisson's ratio cellular solids as Cosserat continua," *J. Eng. Mater. Technol.*, **113**, No. 1, 148–155 (1991).

17. I. Goda, M. Assidi, S. Belouettar, and J. F. Ganghoffer, "A micropolar anisotropic constitutive model of cancellous bone from discrete homogenization," *J. Mech. Behav. Biomed. Mater.*, **16**, 87–108 (2012).

18. I. Goda, M. Assidi, and J. F. Ganghoffer, "A 3D elastic micropolar model of vertebral trabecular bone from lattice homogenization of the bone microstructure," *Biomech. Model. Mechan.*, **13**, No. 1, 53–83 (2014).

19. I. Goda and J. F. Ganghoffer, "Identification of couple-stress moduli of vertebral trabecular bone based on the 3D internal architectures," *J. Mech. Behav. Biomed. Mater.*, **51**, 99–118 (2015).

20. F. dell'Isola, D. Steigmann, and A. Della Corte, "Synthesis of fibrous complex structures: designing microstructure to deliver targeted macroscale response," *Appl. Mech. Rev.*, **67**, No. 6, 060804-060804-21 (2016).

21. F. dell'Isola, I. Giorgio, M. Pawlikowski, and N. L. Rizzi, "Large deformations of planar extensible beams and pantographic lattices: heuristic homogenization, experimental and numerical examples of equilibrium," *Proc. Roy. Soc. A*, **472**, Issue 2185 (2016), DOI: 10.1098/rspa.2015.0790.

22. D. Scerrato, I. Giorgio, N. L. Rizzi, "Three-dimensional instabilities of pantographic sheets with parabolic lattices: numerical investigations," *Z. Angew. Math. Phys.*, **67**, No. 3, 1–19 (2016).

23. D. Scerrato, I. A. Zhurba Eremeeva, T. Lekszycki, and N. L. Rizzi, "On the effect of shear stiffness on the plane deformation of linear second gradient pantographic sheets," *Z. Angew. Math. Mech.* (2016), DOI: 10.1002/zamm.201600066.

24. V. A. Eremeyev and W. Pietraszkiewicz, "Material symmetry group of the non-linear polar-elastic continuum," *Int. J. Solids Struct.*, **49**, No. 14, 1993–2005 (2012).

25. V. A. Eremeyev and W. Pietraszkiewicz, "Material symmetry group and constitutive equations of micropolar anisotropic elastic solids," *Math. Mech. Solids*, **21**, No. 2, 210–221 (2016).

26. T. C. Kennedy and J. B. Kim, "Dynamic stress concentrations in micropolar elastic materials," *Comput. Struct.*, **45**, No. 1, 53–60 (1992).

27. P. Kaloni and T. Ariman, "Stress concentration effects in micropolar elasticity," *Z. Angew. Math. Phys.*, **18**, No. 1, 136–141 (1967).

28. A. R. Khoei, S. Yadegari, and S. O. R. Biabanaki, "3D finite element modeling of shear band localization via the micro-polar Cosserat continuum theory," *Comp. Mater. Sci*., **49**, No. 4, 720–733 (2010).

Received 10. 08. 2016